

Multi-level Metric Learning for Few-shot Image Recognition

Haoxing Chen, Huaxiong Li, Yaohui Li, Chunlin Chen

Nanjing University, Nanjing, China

{haoxingchen, yaohuili}@smail.nju.edu.cn, {huaxiongli, clchen}@nju.edu.cn

Abstract

Few-shot learning is devoted to training a model on few samples. Recently, the method based on local descriptor metric-learning has achieved great performance. Most of these approaches learn a model based on a pixel-level metric. However, such works can only measure the relations between them on a single level, which is not comprehensive and effective. We argue that if query images can simultaneously be well classified via three distinct level similarity metrics, the query images within a class can be more tightly distributed in a smaller feature space, generating more discriminative feature maps. Motivated by this, we propose a novel Multi-level Metric Learning (MML) method for few-shot learning, which not only calculates the pixel-level similarity but also considers the similarity of part-level features and the similarity of distributions. First, we use a feature extractor to get the feature maps of images. Second, a multi-level metric module is proposed to calculate the part-level, pixel-level, and distribution-level similarities simultaneously. Specifically, the distribution-level similarity metric calculates the distribution distance (i.e., Wasserstein distance, Kullback-Leibler divergence) between query images and the support set, the pixel-level, and the part-level metric calculates the pixel-level and part-level similarities respectively. Finally, the fusion layer fuses three kinds of relation scores to obtain the final similarity score. Extensive experiments on popular benchmarks demonstrate that the MML method significantly outperforms the current state-of-the-art methods.

1. Introduction

Humans can learn novel concepts and objects with just a few samples. Recently, many methods were proposed to learn new concepts with limited labeled data, such as semi-supervised learning [40, 35], zero-shot learning [38, 39], and few-shot learning [26, 8, 30, 32, 20, 29, 3]. Facing with the problem of data scarcity, these three paradigms propose solutions from different perspectives. Semi-supervised learning aims to train a model with few labeled data and a

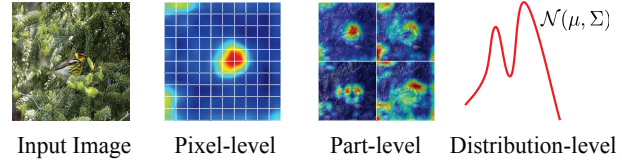


Figure 1. An example of feature representation at different level. (Best view in color.)

large amount of unlabeled data, and zero-shot learning devoted to identifying unseen categories with no labeled data, while few-shot learning focuses on learning new concepts with few labeled data. We propose a novel few-shot learning method to address the problem of data scarcity in this paper.

The few-shot learning methods can be roughly classified into two categories: meta-learning based methods [26, 8, 31] and metric-learning based methods [30, 32, 20, 29, 3]. Metric-based few-shot learning methods have achieved remarkable success due to their fewer parameters and effectiveness. In this work, we focus on this branch.

The basic idea of the metric-learning based few-shot learning method is to learn a good metric to calculate the similarity between query images and the support set. Therefore, how to learn good feature embedding representation and similarity metric are the key problem of metric-learning based few-shot learning method. For feature embedding representation, ProtoNet [30] and RelationNet [32] adopt image-level feature representations. However, due to the scarcity of data, it is not sufficient to measure the relation at the image-level [30, 32]. Recently, CovaMNet [21], DN4 [20] and MATANet [3] introduce local representations (LRs) into few-shot learning and utilize these LRs to represent the image features, which can achieve better recognition results.

For similarity metrics, these existing methods calculate similarities by different metrics. For example, Relation Nets [32] proposes a network to learn the most suitable image-level similarity metric functions. DN4 [3] proposes a cosine-based image-to-class metric to measure the similarity on pixel-level.

However, all methods mentioned above only consider

the distribution of support set, ignoring the natural distribution of query images. We argue that the distribution of the query image is also important for few-shot learning. It is necessary to design a distribution-level similarity metric to capture the distribution-level relations between query images and support set. Moreover, these methods only calculate similarities on a single level, i.e., pixel-level or image-level, which is not effective enough. Intuitively, under the few-shot learning setting, the features obtained by adopting a single similarity measure are not comprehensive, and the single similarity measure may lead to a certain similarity deviation, thus reducing the generalization ability of the model. It is necessary to adopt multi-level similarity metric, generating more discriminative features rather than using a single measure.

To this end, we propose a novel multi-level metric learning method (MML), which can be trained in an end-to-end manner. First, we represent all images as a set of LRs, rather than a global feature representation at the image-level. Moreover, inspired by CBAM [37], we not only consider these features as a pixel-level set but also consider these features as a part-level set. Afterward, we employ a multi-level metric module to calculate the relations at different feature levels as illustrated in Figure 1, i.e., pixel-level, part-level, and distribution-level. Specifically, we use DN4 [20] as the pixel-level similarity metric, to capture local relationships. We propose a novel part-level similarity metric to calculate the different semantic part relations, and employ a distribution similarity metric (i.e., Kullback-Leibler divergence and Wasserstein distance) to get the distribution-level relations. Finally, a fusion layer is proposed to fuse three kinds of relation scores to obtain the final similarity score.

The main contributions are summarized as follows:

- We propose a part-level similarity metric for few-shot learning, which can capture the part-level semantic similarity between query images and support images.
- We propose a novel multi-level metric learning method by computing the semantic similarities on pixel-level, part-level, and distribution-level simultaneously, aiming to find more comprehensive semantic similarities.
- We conduct sufficient experiments on popular benchmark datasets to verify the advancement of our model and the performance of our model achieves the state-of-the-art.

2. Related Works

Recently, the domain of few-shot learning has shown increased interest. In this section, we first review recent metric-learning based few-shot learning methods and then introduce the work that inspire our work.

Metric-learning based few-shot learning: Metric-learning based methods can be roughly classified into two groups:

(1) *Learning feature embedding representation:* Koch et al. [15] used a Siamese Neural Network to tackle the one-shot learning problem, in which the feature extractor is of VGG styled structure and L_1 distance is used to measure the similarity between query images and support images. Snell et al. [30] proposed Prototypical Networks, in which the Euclidean distance is used to compute the distance between class-specific prototypes. Li et al. [20] proposed an image-to-class mechanism to find the relation at pixel-level, in which the image features are represented as a local descriptor collection.

(2) *Learning similarity metric:* Sung et al. [32] replaced the existing metric with the Relation Network, which measures the similarity between each query instance and support classes. Li et al. [20] proposed a Deep Nearest Neighbor Neural Network (DN4) to learn an image-to-class metric by measuring the cosine similarity between the deep local descriptors of a query instance and its neighbors from each support class. Li et al. [21] explored the distribution consistency-based metric by introducing local covariance representation and deep covariance metric. Unlike these methods, the proposed MML measures the similarity at three different feature levels, i.e., pixel-level, part-level, and distribution-level.

Other important works: Woo et al. [37] proposed a Convolutional Block Attention Module (CBAM), which is a kind of attention mechanism module combining spatial information and channel information. According to CBAM, each channel of the feature map can be regarded as a descriptor of a part. Inspired by this, we represent the feature map as a set of part-level feature descriptors and propose a component-level metric to capture semantic correlations between different components.

3. Problem Definition and Formulation

Standard few-shot image recognition problems are often formalized as N -way M -shot classification problem, in which models are given M seen images from each of N classes, and required to correctly classify unseen images. Different from traditional image recognition tasks, few-shot learning aims to classify novel classes after training. This requires that samples used for training, validation, and testing should come from disjoint label space. To be more specific, given a dataset of visual concepts \mathcal{C} , we divide it into three parts: \mathcal{C}_{train} , \mathcal{C}_{val} and \mathcal{C}_{test} , and their label space satisfy $\mathcal{L}_{train} \cap \mathcal{L}_{val} \cap \mathcal{L}_{test} = \emptyset$.

To obtain a trained model, we train our model in an episodic way. That is, in each episode, a new task is randomly sampled from the training set \mathcal{C}_{train} to train the current model. Each task consists of two subsets, includ-

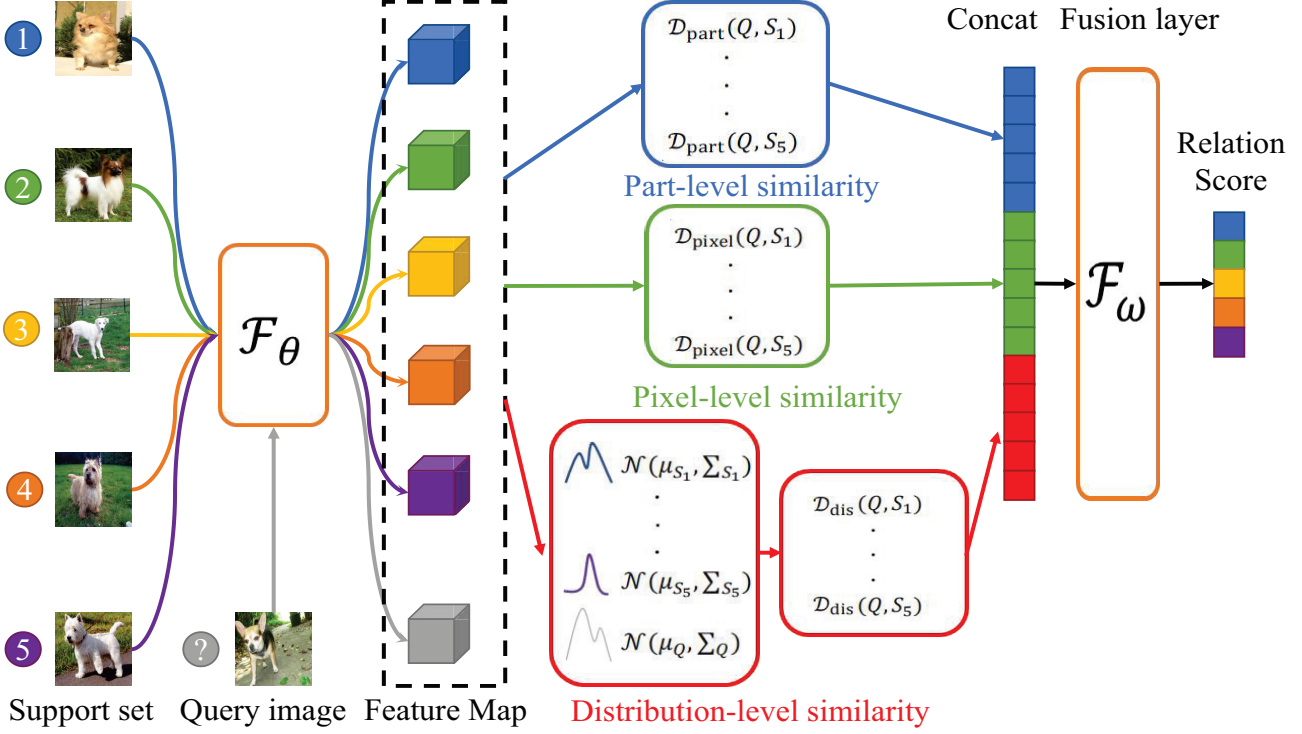


Figure 2. The framework of MML under the 5-way 1-shot image classification setting. The model mainly consists of three modules: the feature extractor \mathcal{F}_θ to learn local representations (LRs), the multi-level metric-learning module to capture the semantic similarity at a different level, i.e., pixel-level, part-level, and distribution-level, and the fusion layer \mathcal{F}_ω to fuse three kinds of relation score to get the final similarity score. (Best view in color.)

ing support set \mathcal{A}_S and query set \mathcal{A}_Q . The \mathcal{A}_S contains \mathcal{N} previously unseen classes, with \mathcal{M} samples for each class. We focus on training our model to correctly determine which category each image in the \mathcal{A}_Q belongs to. Similarly, we randomly sample tasks from \mathcal{C}_{val} and \mathcal{C}_{test} for meta-validation and meta-testing scenarios.

4. Proposed Approach

As shown in Figure 2, our MML is mainly composed of three modules: a feature extractor \mathcal{F}_θ , a multi-level metric-learning module, and a fusion layer \mathcal{F}_ω . All images are first fed into the \mathcal{F}_θ to get feature embeddings. Then, we represented them as pixel-level and part-level feature descriptors. Afterward, the multi-level metric-learning module calculates similarities on part-level, pixel-level, and distribution-level simultaneously. Finally, we adaptively fuse the part-level, pixel-level, and distribution-level similarities together by a fusion layer \mathcal{F}_ω . All the modules can be trained jointly in an end-to-end manner.

4.1. Feature Embedding with Local Representations

As proved by some recent studies [21, 20, 3], feature representation based on local descriptor is more abundant

than image-level feature representation, which can alleviate the problem of sample scarcity. Therefore, we employ local descriptors to represent each image.

Specifically, we employ a feature extractor \mathcal{F}_θ , which can extract informative local descriptors. Given an image X , through \mathcal{F}_θ , we can get a three-dimensional (3D) feature vector $\mathcal{F}_\theta(X) \in \mathbb{R}^{C \times H \times W}$. As proposed by [21, 20, 3], the 3D feature vector can be regarded as a set of HW C -dimensional pixel-level feature descriptors:

$$\mathcal{L}^{\text{pixel}} = \mathcal{F}_\theta(X) = [x_1, \dots, x_{HW}] \in \mathbb{R}^{C \times HW} \quad (1)$$

where x_i is the i -th pixel-level feature descriptor.

Inspired by [37, 11], each channel in $\mathcal{F}_\theta(X)$ can be regarded as a semantic representation of a specific part in the image, as shown in Figure 1(b). Therefore, the 3D feature vector can also be regarded as a set of C HW -dimensional part-level feature descriptors:

$$\mathcal{L}^{\text{part}} = \mathcal{F}_\theta(X) = [x_1, \dots, x_C] \in \mathbb{R}^{HW \times C} \quad (2)$$

where x_j is the j -th part-level feature descriptor.

4.2. Multi-level Metric Learning

Under N -way M -shot few-shot learning setting, given a query image Q and a certain support class S , through

feature extractor \mathcal{F}_θ , we can get the feature representation $\mathcal{F}_\theta(Q) \in \mathbb{R}^{C \times H \times W}$ and $\mathcal{F}_\theta(S) \in \mathbb{R}^{M \times C \times H \times W}$, respectively. The $\mathcal{F}_\theta(Q)$ can be regarded as

$$\mathcal{L}_Q^{\text{pixel}} = [u_1^{\text{pixel}}, \dots, u_{HW}^{\text{pixel}}] \in \mathbb{R}^{C \times HW} \quad (3)$$

$$\mathcal{L}_Q^{\text{part}} = [u_1^{\text{part}}, \dots, u_C^{\text{part}}] \in \mathbb{R}^{HW \times C} \quad (4)$$

Also, the $\mathcal{F}_\theta(S)$ can be regarded as

$$\mathcal{L}_S^{\text{pixel}} = [v_1^{\text{pixel}}, \dots, v_{MHW}^{\text{pixel}}] \in \mathbb{R}^{C \times MHW} \quad (5)$$

$$\mathcal{L}_S^{\text{part}} = [v_1^{\text{part}}, \dots, v_{MC}^{\text{part}}] \in \mathbb{R}^{HW \times MC} \quad (6)$$

Part-level similarity metric. After obtaining the part-level feature representation of the query image Q and the support class S , we calculate the correlation matrix $R^{\text{part}} \in \mathbb{R}^{C \times MC}$ between the query image and the support class on part-level:

$$\mathcal{R}_{i,j}^{\text{part}} = \cos(u_i^{\text{part}}, v_j^{\text{part}}) \quad (7)$$

$$\cos(u_i^{\text{part}}, v_j^{\text{part}}) = \frac{(u_i^{\text{part}})^T v_j^{\text{part}}}{\|u_i^{\text{part}}\| \cdot \|v_j^{\text{part}}\|} \quad (8)$$

where $i \in \{1, \dots, C\}, j \in \{1, \dots, MC\}$, $\mathcal{R}_{i,j}^{\text{part}}$ is (i, j) element of $\mathcal{R}^{\text{part}}$ reflecting the distance between the i -th part-level feature descriptor of the query image and the j -th part-level feature descriptor of support class and $\cos(\cdot, \cdot)$ is Cosine similarity function. Each row in $\mathcal{R}^{\text{part}}$ represents the semantic relation of each part-level feature descriptor in the query image to all part-level feature descriptors of all images in the support class. For each part-level feature descriptor u_i^{part} of the query image Q , we find its ξ most similar part-level feature descriptors. Then, we sum $C \times \xi$ selected part-level feature descriptors as the part-level similarity between the query image and the support class

$$\mathcal{D}_{\text{part}}(Q, S) = \text{Top}\xi(\mathcal{R}_i^{\text{part}}) \quad (9)$$

where $\text{Top}\xi(\cdot)$ means selecting the ξ largest elements in each row of the $\mathcal{R}^{\text{part}}$.

Typically, ξ is set as 1 in our work.

Pixel-level similarity metric We adopt DN4 [20] as our pixel-level similarity metric, which proposed an image-to-class measure to capture the local relations between query images and support class. Here, we have a brief review of DN4. Given a query image and a support class, we can get their pixel-level feature set $\mathcal{L}_Q^{\text{pixel}}$ and $\mathcal{L}_S^{\text{pixel}}$. Then, we calculate the correlation matrix R^{pixel} between the query image and the support class on pixel-level and select the k largest element in each row of the correlation matrix:

$$\mathcal{R}_{i,j}^{\text{pixel}} = \cos(u_i^{\text{pixel}}, v_j^{\text{pixel}}) \quad (10)$$

$$\cos(u_i^{\text{pixel}}, v_j^{\text{pixel}}) = \frac{(u_i^{\text{pixel}})^T v_j^{\text{pixel}}}{\|u_i^{\text{pixel}}\| \cdot \|v_j^{\text{pixel}}\|} \quad (11)$$

$$\mathcal{D}_{\text{pixel}}(Q, S) = \text{Top}k(\mathcal{R}_i^{\text{pixel}}) \quad (12)$$

Typically, k is set as 1 in our work.

Distribution-level similarity metric Inspired by [21], we assume the distribution of pixel-level feature descriptors are multivariate Gaussian. Therefore, we can use $Q = \mathcal{N}(\mu_Q, \Sigma_Q)$ and $S = \mathcal{N}(\mu_S, \Sigma_S)$ as the query image's distribution and the support class's distribution, respectively. $\mu \in \mathbb{R}^C$ indicate the mean vector and $\Sigma \in \mathbb{R}^{C \times C}$ indicate covariance matrix of a specific distribution. Then the distribution-level metric can be denoted as

$$\mathcal{D}_{\text{dis}}(Q, S) = \mathcal{F}(Q, S) \quad (13)$$

where $\mathcal{F}(\cdot)$ is a certain distribution metric. There are many options for distance metric function. In this paper, Kullback-Leibler divergence [17] and Wasserstein distance are selected for experiments:

(1) *Kullback-Leibler divergence*: We use KL divergence to match the distribution of Q to the one of support class S , so the KL divergence can be denoted as

$$\mathcal{F}_{\text{KL}}(S||Q) = \frac{1}{2} \left(\text{trace}(\Sigma_Q^{-1} \Sigma_S) + \ln \left(\frac{\det \Sigma_Q}{\det \Sigma_S} \right) + (\mu_Q - \mu_S)^T \Sigma_Q^{-1} (\mu_Q - \mu_S) - c \right) \quad (14)$$

where \det is the value of the determinant of a square matrix, $\text{trace}(\cdot)$ denotes the trace operation of matrixes.

(2) *Wasserstein distance*: 2-Wasserstein distance can also be taken as a choice of $\mathcal{F}(\cdot)$, whose formulation is defined as follows

$$\mathcal{F}_{\text{Wass}}(Q, S) = \|\mu_Q - \mu_S\|_2^2 + \text{trace} \left(\Sigma_Q + \Sigma_S - 2(\Sigma_Q^{\frac{1}{2}} \Sigma_S \Sigma_Q^{\frac{1}{2}})^{\frac{1}{2}} \right) \quad (15)$$

However, since the square root of the matrix incurs huge computational time, we use the approximate form proposed by [10]:

$$\mathcal{F}_{\text{Wass}}(Q, S) = \|\mu_Q - \mu_S\|_2^2 + \|\Sigma_Q - \Sigma_S\|_F^2 \quad (16)$$

4.3. Fusion Layer

Since three different level similarities have been calculated, i.e., part-level, pixel-level, and distribution-level, we need to design a fusion module to integrate them. In order to tackle this problem, we adopt an adaptive fusion strategy, which use a learnable vector $w = [w_1, w_2, w_3]$ to integrate these three parts. Specifically, the final similarity can be obtained by the following equation

$$\mathcal{D}(Q, S) = w_1 \cdot \mathcal{D}_{\text{part}}(Q, S) + w_2 \cdot \mathcal{D}_{\text{pixel}}(Q, S) - w_3 \cdot \mathcal{D}_{\text{dis}}(Q, S) \quad (17)$$

Note that since the distribution level measure represents difference rather than sameness, we use negative numbers

Dataset	N_{all}	N_{train}	N_{val}	N_{test}
<i>mini</i> ImageNet	100	64	16	20
<i>tiered</i> ImageNet	608	351	97	160
Stanford Dogs	120	70	20	30
Stanford Cars	196	130	17	49
CUB Birds	200	100	50	50

Table 1. The splits of evaluation datasets. N_{all} is the number of all classes. N_{train} , N_{val} and N_{test} indicate the number of classes in training set, validation set and test set.

to indicate similarity. Under the 5-way 1-shot few-shot learning setting, input a query image, we will get five-dimensional vectors on each level. We first concatenate these three vectors and balance the size of these three vectors by a Batch Normalization layer. Then, we use a 1D convolution layer with the kernel size of 1×1 and the dilation value of 3. Finally, we can get a weighted 5-dimensional similarity vector \mathcal{P} , we use it for final classification.

5. Experiments

In this section, we perform extensive experiments to verify the advance and effectiveness of MML.

5.1. Datasets

To verify the advance and effectiveness of our proposed MML, we performed experiments on five benchmark datasets: *mini*ImageNet [8], *tiered*ImageNet [27], CUB Birds [34], Stanford Dogs [13] and StanfordCars [16].

ImageNet derivatives: Both *mini*ImageNet dataset and *tiered*ImageNet dataset are subsets of ImageNet [6]. The *mini*ImageNet dataset consists 100 classes, each of which contains 600 samples, and the *tiered*ImageNet contains 608 classes.

Fine-grained dataset: CUB Birds contains 11,788 images of 200 classes of birds. Stanford Dogs contains 20,580 annotated images from 120 dog species. Stanford Cars including 16,185 annotated images of 196 breeds of cars.

The partition of all data sets is shown in Table 1. All images are resized to 84×84 .

5.2. Network Architecture

In order to make a fair comparison with other works, we adopt the shallow *Conv64F* network [21, 20] and *ResNet-12* network [18] as our feature extractor \mathcal{F}_θ .

Conv64F has four convolution blocks, each convolutional block consists of a convolutional layer with $64 \times 3 \times 3$ filters, a batch normalization layer, and a Leaky ReLU activation layer. Besides, the 2×2 max-pooling layer is added in the first two blocks.

ResNet-12 has four residual blocks, each residual block has 3 convolutional layers with 3×3 kernel, and a 2×2 max-pooling layer is added in the first residual block.

5.3. Implementation Details

We use pytorch [25] to implement all the experiments¹. We conduct our experiments on a series of N -way M -shot tasks, i.e., 5-way 1-shot and 5-way 5-shot. On ImageNet derivatives and fine-grained datasets, we train our model 50 epochs. In each epoch, we randomly sampled 10000 tasks. We use the Adam [14] optimizer and the cross-entropy (CE) loss to train our MML. Our batch size is set to 4, the initial learning rate is 0.001, and multiplied by 0.5 every 10 epochs. During the test stage, we report our performance based on an average of 1000 tasks. We report the average accuracy as well as the corresponding 95% confidence interval over these 1000 tasks.

As we all know, using deeper networks to extract features or using pre-trained models can achieve higher accuracy. To make a fair comparison, following the previous works, when using *Conv-64F* as feature extractor \mathcal{F}_θ , we do not apply the pre-training strategy. And when *ResNet-12* is used as feature extractor \mathcal{F}_θ , we apply an additional pre-training strategy as suggested in [22].

5.4. Comparison Against Related Approaches

Results on ImageNet derivatives. As seen from Table 2, when adopting *Conv-64F* as feature extractor, our MML(KL) achieves the highest accuracy on *mini*ImageNet with 55.14% and 73.33% on 5-way 1-shot and 5-way 5-shot tasks respectively, which make a great improvement compared to the previous pixel-level metric-learning based methods. For example, our MML(KL) is 7.7% and 7.6% better than CovaMNet and DN4 on the 5-way 1-shot task, respectively. Although the experimental results of MML(Wasserstein) are not as good as MML(KL), MML(Wasserstein) is also better than other methods. Moreover, when adopting *ResNet-12* as feature extractor, our MML(KL) achieves 65.55% and 81.86% in 5-way 1-shot and 5-way 5-shot respectively, which achieves competitive performance.

Table 3 summarizes the results on the *tiered*ImageNet dataset. Our results outperform the state-of-the-art by a significant margin. For example, with *Conv-64F* feature extractor, our MML(Wass) achieves new state-of-the-art results on *tiered*ImageNet benchmark (57.89% - up 5.3% over the previous best) on 5-way 1-shot and (75.49% - up 1.4% over the previous best) on 5-way 5-shot.

Results on fine-grained datasets. Table 4 evaluates our method on three fine-grained datasets, i.e., Stanford Dogs, Stanford Cars, and CUB Birds. It can be seen that the proposed MML obtains significant improvements compared with previous state-of-the-art methods. For the 5-way 1-shot task, the proposed MML(KL) obtains state-of-the-art performance on all three fine-grained datasets. And for the

¹Our code is available at <https://github.com/chenhaoxing/M2L>.

Method	Venue	Backbone	Type	5-way 1-shot	5-way 5-shot
MAML+L2F [2]	CVPR'20	Conv-32F	Meta	52.10±0.49	69.38±0.46
WarpGrad [9]	ICLR'20	Conv-32F	Meta	52.30±0.80	68.40±0.60
BOIL [24]	ICLR'21	Conv-64F	Meta	49.61±0.16	66.45±0.37
MatchingNet [33]	NeurIPS'16	Conv-64F	Metric	43.56±0.84	55.31±0.73
ProtoNet [30]	NeurIPS'17	Conv-64F	Metric	49.42±0.78	68.20±0.66
RelationNet [32]	CVPR'18	Conv-64F	Metric	50.44±0.82	65.32±0.70
CovaMNet [21]	AAAI'19	Conv-64F	Metric	51.19±0.76	67.65±0.63
DN4 [20]	CVPR'19	Conv-64F	Metric	51.24±0.74	71.02±0.64
CTM* [19]	CVPR'19	Conv-64F	Metric	41.62±0.00	58.77±0.00
DSN [29]	CVPR'20	Conv-64F	Metric	51.78±0.96	68.99±0.69
Align(Centroid) [1]	ECCV'20	Conv-64F	Metric	53.14±1.06	71.45±0.72
Neg-Margin [22]	ECCV'20	Conv-64F	Others	52.68±0.76	70.41±0.66
Two-stage [5]	T-IP'2020	Conv-64F	Others	52.68±0.51	70.91±0.85
MML(KL)	Ours	Conv-64F	Metric	55.14±0.63	73.33±0.50
MML(Wass)	Ours	Conv-64F	Metric	54.94±0.64	72.81±0.50
ProtoNet [30]	NeurIPS'17	ResNet-12	Metric	60.37±0.83	78.02 ±0.57
CTM [19]	CVPR'19	ResNet-12	Metric	64.12±0.82	80.51±0.13
DSN [29]	CVPR'20	ResNet-12	Metric	62.64±0.66	78.73±0.45
MetaOptNet [18]	CVPR'19	ResNet-12	Others	62.64±0.61	78.63±0.46
Neg-Margin [22]	ECCV'20	ResNet-12	Others	63.85±0.81	81.57±0.56
DeepEMD [41]	CVPR'20	ResNet-12	Metric	65.91±0.82	79.74±0.56
MML(KL)	Ours	ResNet-12	Metric	65.55±0.77	81.86±0.51
MML(Wass)	Ours	ResNet-12	Metric	65.32±0.76	81.77±0.53

Table 2. Comparison with other state-of-the-art methods with 95% confidence intervals on *miniImageNet*. The third column shows which kind of embedding is employed. The fourth column shows which type of the method belongs to, i.e., meta-learning based, metric-learning based, and other kinds of methods. (Top two performances are shown in red and blue.)

Model	Backbone	5-Way Accuracy(%)	
		1-shot	5-shot
ProtoNet [30]	Conv-64F	48.67±0.87	69.57±0.75
RelationNet [32]	Conv-64F	54.48±0.93	71.32±0.78
CovaMNet [21]	Conv-64F	54.98±0.90	71.51±0.75
DN4 [20]	Conv-64F	53.37±0.86	74.45±0.70
MELR [7]	Conv-64F	56.38±0.48	73.22±0.41
MML(KL)	Conv-64F	57.37±0.70	74.98±0.55
MML(Wass)	Conv-64F	57.89±0.69	75.49±0.55
ProtoNet [30]	ResNet-12	68.37±0.23	83.43±0.16
RelationNet [32]	ResNet-12	58.99±0.86	75.78±0.76
DSN [29]	ResNet-12	67.39±0.82	82.85±0.56
DeepEMD [41]	ResNet-12	71.16±0.87	83.95±0.58
MML(KL)	ResNet-12	71.32±0.75	84.15±0.59
MML(Wass)	ResNet-12	71.82±0.76	84.53±0.61

Table 3. Comparison with other state-of-the-art methods with 95% confidence intervals on *tieredImageNet*. (Top two performances are shown in red and blue.)

5-way 5-shot task, the proposed MML(KL) also achieves state-of-the-art performance on Stanford Dogs and Stanford

Car, and a comparable performance on CUB Birds. Specifically, compared with pixel-level metric-learning based methods (i.e., CovaMNet, DN4, and LRPABN), MML(KL) is 20.3%, 20.2%, and 0.4% better than the best one of them on Stanford Dogs, Stanford Cars, and CUB Birds under 5-way 1-shot setting.

The reason why our MML can achieve these state-of-the-art performances is that MML can measure the semantic similarities on multiple levels, i.e., part-level, pixel-level, and distribution-level.

5.5. Cross-Domain Few-Shot Learning

Cross-domain few-shot learning assumes that images in the training set and test set can come from different domains. We proceed by meta-training the models on the *miniImageNet* training set and evaluate the model on three fine-grained test sets. This setting of domain shift results in a large margin between the distribution of training set and test set. We use the same dataset partitioning as shown in Table 1. To verify the effectiveness of our model, we compared five classical metric-learning based few-shot learning methods: MatchingNet, ProtoNet, RelationNet, CovaMNet, and DN4.

Model	5-Way Accuracy(%)					
	Stanford Dogs		Stanford Cars		CUB Birds	
	1-shot	5-shot	1-shot	5-shot	1-shot	5shot
MatchingNet [33]	35.80±0.99	47.50±1.03	34.80±0.98	44.70±1.03	61.16±0.89	72.86±0.70
ProtoNet [30]	37.59±1.00	48.19±1.03	40.90±1.01	52.93±1.03	51.31±0.91	70.77±0.69
GNN [28]	46.98±0.98	62.27±0.95	55.85±0.97	71.25±0.89	51.83±0.98	63.69±0.94
MAML [8]	44.81±0.34	58.68±0.31	47.22±0.39	61.21±0.28	55.92±0.95	72.09±0.76
RelationNet [32]	43.33±0.42	55.23±0.41	47.67±0.47	60.59±0.40	62.45±0.98	76.11±0.69
adaCNN [23]	41.87±0.42	53.93±0.44	42.14±0.41	50.12±0.34	56.57±0.47	61.21±0.42
PCM [36]	28.78±2.33	46.92±2.00	29.63±2.38	52.28±1.46	42.10±1.96	62.48±1.21
CovaMNet [21]	49.10±0.76	63.04±0.65	56.65±0.86	71.33±0.62	60.58±0.69	74.24±0.68
DN4 [20]	45.41±0.76	63.51±0.62	59.84±0.80	88.65±0.44	52.79±0.86	81.45±0.70
PABN _{+cpt} [12]	45.65±0.71	61.24±0.62	54.44±0.71	67.36±0.61	63.56±0.79	75.35±0.58
LRPABN _{+cpt} [12]	45.72±0.75	60.94±0.66	60.28±0.76	73.29±0.58	63.63±0.77	76.06±0.58
MML(KL)	59.05±0.68	75.59±0.51	72.43±0.65	91.05±0.30	63.86±0.67	80.73 ±0.46
MML(Wass)	58.07±0.68	75.15±0.49	72.40±0.63	91.01±0.31	63.64±0.69	80.63 ±0.47

Table 4. Experimental results compared with other methods on three fine-grained datasets. (Backbone: Conv-64F. Top two performances are shown in red and blue.)

Model	5-Way Accuracy(%)					
	<i>miniImageNet</i> →Dogs		<i>miniImageNet</i> →Cars		<i>miniImageNet</i> →Birds	
	1-shot	5-shot	1-shot	5-shot	1-shot	5shot
MatchingNet [33]	31.53±0.98	41.25±1.03	24.88±0.95	40.55±0.98	33.75±0.95	53.14±0.77
ProtoNet [30]	33.24±0.99	42.16±1.02	31.47±1.03	48.75±1.02	42.09±0.88	62.02±0.65
RelationNet [32]	31.99±0.55	50.35±0.49	37.14±0.51	44.95±0.43	38.25±0.99	57.73±0.76
CovaMNet [21]	38.03±0.77	56.22±0.63	32.33±0.75	49.86±0.63	43.11±0.65	63.22±0.69
DN4 [20]	38.37±0.72	56.50±0.72	32.51±0.62	50.19±0.73	43.65±0.77	63.78±0.69
MML(KL)	40.94±0.57	58.43±0.54	34.05±0.51	53.19±0.56	44.86±0.58	65.20±0.56
MML(Wass)	41.26±0.60	57.73±0.57	34.22±0.50	52.80±0.54	44.63±0.58	64.98±0.52

Table 5. Experimental results compared with other methods on *miniImageNet* under cross-domain few-shot learning setting. (Backbone: Conv-64F. Top two performances are shown in red and blue.)

Table 5 gives the quantitative results. It can be seen that MML outperforms all the baseline methods. This verifies that our model is more robust under these more challenging tasks. The reason why our MML can achieve these results is that our MML can capture more comprehensive semantic similarities than previous metric-learning based methods.

5.6. Ablation Study

To further explore the effect of the multi-level metric learning module, we prune any of three similarity branches in the multi-level metric-learning module. Specifically, we remove one or two branches from the multi-level metric-learning module and experiment on the *miniImageNet* and *tieredImageNet* datasets.

As seen in Table 6, each part of the MML is indispensable. It can be observed that the accuracy of few-shot image recognition using only one level of features is very low. The results were significantly improved when two or three lev-

els of features were used together, and the results were best when all three levels were used together. Specifically, compared with the method that only using pixel-level features, our MML gains 7.6% and 3.1% improvements.

5.7. Complexity Analysis

As shown in Table 7, we compare the trainable parameters to prove that our model is both simple and effective. Although our multi-level metric-learning module has three branches, each branch has no trainable parameters. Therefore, if we ignore three trainable parameters in the fusion layer, our MML is non-parametric if not considering the feature extractor \mathcal{F}_θ . Our model achieved a great improvement in accuracy while maintaining the same number of trainable parameters as MatchingNet, ProtoNet, CovaMNet, and DN4. Specifically, on the Stanford Dogs dataset, our MML(KL) obtains 64.9%, 57.1%, 20.3% and 30.0% improvements over MatchingNet, ProtoNet, CovaM-

Part	Pixel	Dis.(KL)	Dis.(Wass)	5-Way Accuracy(%)			
				<i>miniImageNet</i>		<i>tieredImageNet</i>	
				1-shot	5-shot	1-shot	5-shot
✓				49.82±0.65	65.33±0.98	51.04±0.93	70.25±1.13
	✓			51.32±0.73	70.95±0.67	53.22±0.85	74.33±0.71
		✓		52.87±0.64	69.32±0.50	55.43±0.68	74.21±0.56
			✓	50.31±0.62	67.62±0.53	52.88±0.71	73.67±0.57
✓	✓			51.95±0.68	71.35±0.65	53.65±0.87	74.43±0.76
✓		✓		53.15±0.62	70.16±0.53	55.74±0.71	74.07±0.55
✓			✓	51.33±0.65	68.56±0.55	53.62±0.76	74.32±0.59
	✓	✓		53.82±0.63	72.13±0.50	55.69±0.71	74.46±0.56
	✓		✓	53.42±0.59	72.08±0.52	54.85±0.68	73.85±0.53
✓	✓	✓		55.14±0.63	73.12±0.69	57.37±0.70	74.98±0.55
✓	✓		✓	54.94±0.64	72.81±0.50	57.89±0.69	75.49±0.55

Table 6. Ablation study on *miniImageNet*. (Backbone: Conv-64F.)

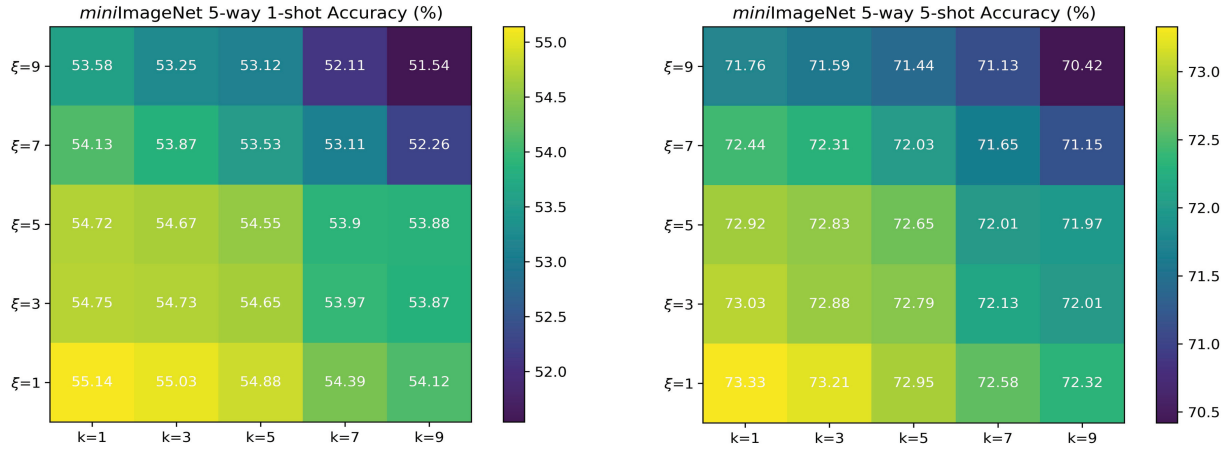


Figure 3. Influence of superparameters ξ and k .

Model	Params	5-Way Accuracy(%)	
		1-shot	5-shot
MatchingNet [33]	0.113M	35.80±0.99	47.50±1.03
ProtoNet [30]	0.113M	37.59±1.00	48.19±1.03
RelationNet [32]	0.229M	43.33±0.42	55.23±0.41
GNN [28]	1.619M	46.98±0.98	62.27±0.95
CovaMNet [21]	0.113M	49.10±0.76	63.04±0.65
DN4 [20]	0.113M	45.41±0.76	63.51±0.62
MML(KL)	0.113M	59.05±0.68	75.59±0.51
MML(Wass)	0.113M	58.07±0.68	75.15±0.49

Table 7. The number of trainable parameters in different models and the corresponding classification accuracies on Stanford Dogs. (Backbone: Conv-64F. Top two performances are shown in red and blue.)

Net, and DN4 under the 5-way 1-shot few-shot learning setting, respectively. Moreover, on the 5-way 5-shot task, our MML(KL) obtains 59.1%, 56.9%, 19.9% and 19.0% im-

provements over MatchingNet, ProtoNet, CovaMNet, and DN4 respectively.

5.8. Influence of Superparameter ξ and k .

In the part-level and pixel-level similarity metrics, we need to choose suitable ξ and k . For this purpose, we conduct a contrast experiment on *miniImageNet* dataset under both 5-way 1-shot and 5-way 5-shot settings by varying the value of $\xi \in \{1, 3, 5, 7, 9\}$ and the value of $k \in \{1, 3, 5, 7, 9\}$. Experimental results are shown in Figure 3. It can be seen that when $\xi = 1$ and $k = 1$, the experimental result of MML(KL) is the best.

6. Conclusion

In this paper, we revisit the metric-learning based method and proposed a novel Multi-level Metric Learning (MML) method for few-shot image recognition, aiming to capture more comprehensive semantic similarities. Specifically, the MML can measure the semantic similarities on

multiple levels and produce more discriminative features. Extensive experiments show the effectiveness and the superiority of the MML.

References

- [1] Arman Afrasiyabi, Jean-François Lalonde, and Christian Gagné. Associative alignment for few-shot image classification. In *Proc. Eur. Conf. Comput. Vis. (ECCV)*, volume 12350, pages 18–35, 2020.
- [2] Sungyong Baik, Seokil Hong, and Kyoung Mu Lee. Learning to forget for meta-learning. In *Proc. IEEE Conf. Comput. Vis. Pattern Recognit. (CVPR)*, pages 2376–2384, 2020.
- [3] Haoxing Chen, Huaxiong Li, Yaohui Li, and Chunlin Chen. Multi-scale adaptive task attention network for few-shot learning. *arXiv preprint arXiv:2011.14479*, 2020.
- [4] Wei-Yu Chen, Yen-Cheng Liu, Zsolt Kira, Yu-Chiang Frank Wang, and Jia-Bin Huang. A closer look at few-shot classification. In *Proc. Int. Conf. Learn. Represent. (ICLR)*, 2019.
- [5] Debasmit Das and C. S. George Lee. A two-stage approach to few-shot learning for image recognition. *IEEE Trans. Image Process.*, 29:3336–3350, 2020.
- [6] Jia Deng, Wei Dong, Richard Socher, Li-Jia Li, Kai Li, and Fei-Fei Li. Imagenet: A large-scale hierarchical image database. In *Proc. IEEE Conf. Comput. Vis. Pattern Recognit. (CVPR)*, pages 248–255, 2009.
- [7] Nanyi Fei, Zhiwu Lu, Tao Xiang, and Songfang Huang. Melr: Meta-learning via modeling episode-level relationships for few-shot learning. In *Proc. Int. Conf. Learn. Represent. (ICLR)*, 2021.
- [8] Chelsea Finn, Pieter Abbeel, and Sergey Levine. Model-agnostic meta-learning for fast adaptation of deep networks. In *Proc. Int. Conf. Mach. Learn. (ICML)*, volume 70, pages 1126–1135, 2017.
- [9] Sebastian Flennerhag, Andrei A. Rusu, Razvan Pascanu, Francesco Visin, Hujun Yin, and Raia Hadsell. Meta-learning with warped gradient descent. In *Proc. Int. Conf. Learn. Represent. (ICLR)*, 2020.
- [10] Ran He, Xiang Wu, Zhenan Sun, and Tieniu Tan. Wasserstein CNN: learning invariant features for NIR-VIS face recognition. *IEEE Trans. Pattern Anal. Mach. Intell.*, 41(7):1761–1773, 2019.
- [11] Jie Hu, Li Shen, and Gang Sun. Squeeze-and-excitation networks. In *Proc. IEEE Conf. Comput. Vis. Pattern Recognit. (CVPR)*, pages 7132–7141, 2018.
- [12] Huaxi Huang, Junjie Zhang, Jian Zhang, Jingsong Xu, and Qiang Wu. Low-rank pairwise alignment bilinear network for few-shot fine-grained image classification. *arXiv preprint arXiv:1908.01313*, 2019.
- [13] Aditya Khosla, Nityananda Jayadevaprakash, Bangpeng Yao, and Fei-Fei Li. Novel dataset for fine-grained image categorization: Stanford dogs. In *Proc. CVPR Workshops (CVPRW)*, volume 2, 2011.
- [14] Diederik P. Kingma and Jimmy Ba. Adam: A method for stochastic optimization. In *Proc. Int. Conf. Learn. Represent. (ICLR)*, 2015.
- [15] Gregory Koch, Richard Zemel, and Ruslan Salakhutdinov. Siamese neural networks for one-shot image recognition. In *Proc. ICML Workshops (ICMLW)*, volume 2, 2015.
- [16] Jonathan Krause, Michael Stark, Jia Deng, and Li Fei-Fei. 3d object representations for fine-grained categorization. In *Proc. ICCV Workshops (ICCVW)*, pages 554–561, 2013.
- [17] S. Kullback and R. A. Leibler. On information and sufficiency. *Ann. Math. Statist.*, 22:79–86, 1951.
- [18] Kwonjoon Lee, Subhansu Maji, Avinash Ravichandran, and Stefano Soatto. Meta-learning with differentiable convex optimization. In *Proc. IEEE Conf. Comput. Vis. Pattern Recognit. (CVPR)*, pages 10657–10665, 2019.
- [19] Hongyang Li, David Eigen, Samuel Dodge, Matthew Zeiler, and Xiaogang Wang. Finding task-relevant features for few-shot learning by category traversal. In *Proc. IEEE Conf. Comput. Vis. Pattern Recognit. (CVPR)*, pages 1–10, 2019.
- [20] Wenbin Li, Lei Wang, Jinglin Xu, Jing Huo, Yang Gao, and Jiebo Luo. Revisiting local descriptor based image-to-class measure for few-shot learning. In *Proc. IEEE Conf. Comput. Vis. Pattern Recognit. (CVPR)*, pages 7260–7268, 2019.
- [21] Wenbin Li, Jinglin Xu, Jing Huo, Lei Wang, Yang Gao, and Jiebo Luo. Distribution consistency based covariance metric networks for few-shot learning. In *Proc. AAAI Conf. Artif. Intell. (AAAI)*, pages 8642–8649, 2019.
- [22] Bin Liu, Yue Cao, Yutong Lin, Qi Li, Zheng Zhang, Ming-sheng Long, and Han Hu. Negative margin matters: Understanding margin in few-shot classification. In *Proc. Eur. Conf. Comput. Vis. (ECCV)*, volume 12349, pages 438–455, 2020.
- [23] Tsendsuren Munkhdalai, Xingdi Yuan, Soroush Mehri, and Adam Trischler. Rapid adaptation with conditionally shifted neurons. In Jennifer G. Dy and Andreas Krause, editors, *Proc. Int. Conf. Mach. Learn. (ICML)*, volume 80, pages 3661–3670, 2018.
- [24] Jaehoon Oh, Hyungjun Yoo, ChangHwan Kim, and Se-Young Yun. Boil: Towards representation change for few-shot learning. In *Proc. Int. Conf. Learn. Represent. (ICLR)*, 2021.
- [25] Adam Paszke, Sam Gross, Francisco Massa, Adam Lerer, James Bradbury, Gregory Chanan, Trevor Killeen, Zeming Lin, Natalia Gimelshein, Luca Antiga, Alban Desmaison, Andreas Köpf, Edward Yang, Zachary DeVito, Martin Raison, Alykhan Tejani, Sasank Chilamkurthy, Benoit Steiner, Lu Fang, Junjie Bai, and Soumith Chintala. Pytorch: An imperative style, high-performance deep learning library. In *Proc. Adv. Neural Inf. Process. Syst. (NeurIPS)*, pages 8024–8035, 2019.
- [26] Sachin Ravi and Hugo Larochelle. Optimization as a model for few-shot learning. In *Proc. Int. Conf. Learn. Represent. (ICLR)*, 2017.
- [27] Mengye Ren, Eleni Triantafillou, Sachin Ravi, Jake Snell, Kevin Swersky, Joshua B. Tenenbaum, Hugo Larochelle, and Richard S. Zemel. Meta-learning for semi-supervised few-shot classification. In *Proc. Int. Conf. Learn. Represent. (ICLR)*, 2018.
- [28] Victor Garcia Satorras and Joan Bruna Estrach. Few-shot learning with graph neural networks. In *Proc. Int. Conf. Learn. Represent. (ICLR)*, 2018.

- [29] Christian Simon, Piotr Koniusz, Richard Nock, and Mehrtaash Harandi. Adaptive subspaces for few-shot learning. In *Proc. IEEE Conf. Comput. Vis. Pattern Recognit. (CVPR)*, pages 4135–4144, 2020.
- [30] Jake Snell, Kevin Swersky, and Richard S. Zemel. Prototypical networks for few-shot learning. In *Proc. Adv. Neural Inf. Process. Syst. (NeurIPS)*, pages 4077–4087, 2017.
- [31] Qianru Sun, Yaoyao Liu, Tat-Seng Chua, and Bernt Schiele. Meta-transfer learning for few-shot learning. In *Proc. IEEE Conf. Comput. Vis. Pattern Recognit. (CVPR)*, pages 403–412, 2019.
- [32] Flood Sung, Yongxin Yang, Li Zhang, Tao Xiang, Philip H. S. Torr, and Timothy M. Hospedales. Learning to compare: Relation network for few-shot learning. In *Proc. IEEE Conf. Comput. Vis. Pattern Recognit. (CVPR)*, pages 1199–1208, 2018.
- [33] Oriol Vinyals, Charles Blundell, Tim Lillicrap, Koray Kavukcuoglu, and Daan Wierstra. Matching networks for one shot learning. In *Proc. Adv. Neural Inf. Process. Syst. (NeurIPS)*, pages 3630–3638, 2016.
- [34] Catherine Wah, Steve Branson, Peter Welinder, Pietro Perona, and Serge Belongie. The caltech-ucsd birds-200-2011 dataset. 2011.
- [35] Yaxing Wang, Salman Khan, Abel Gonzalez-Garcia, Joost van de Weijer, and Fahad Shahbaz Khan. Semi-supervised learning for few-shot image-to-image translation. In *Proc. IEEE Conf. Comput. Vis. Pattern Recognit. (CVPR)*, pages 4452–4461, 2020.
- [36] Xiu-Shen Wei, Peng Wang, Lingqiao Liu, Chunhua Shen, and Jianxin Wu. Piecewise classifier mappings: Learning fine-grained learners for novel categories with few examples. *IEEE Trans. Image Process.*, 28(12):6116–6125, 2019.
- [37] Sanghyun Woo, Jongchan Park, Joon-Young Lee, and In So Kweon. CBAM: convolutional block attention module. In *Proc. Eur. Conf. Comput. Vis. (ECCV)*, volume 11211, pages 3–19, 2018.
- [38] Jiamin Wu, Tianzhu Zhang, Zheng-Jun Zha, Jiebo Luo, Yongdong Zhang, and Feng Wu. Self-supervised domain-aware generative network for generalized zero-shot learning. In *Proc. IEEE Conf. Comput. Vis. Pattern Recognit. (CVPR)*, pages 12764–12773, 2020.
- [39] Yunlong Yu, Zhong Ji, Jungong Han, and Zhongfei Zhang. Episode-based prototype generating network for zero-shot learning. In *Proc. IEEE Conf. Comput. Vis. Pattern Recognit. (CVPR)*, pages 14032–14041, 2020.
- [40] Zhongjie Yu, Lin Chen, Zhongwei Cheng, and Jiebo Luo. Transmatch: A transfer-learning scheme for semi-supervised few-shot learning. In *Proc. IEEE Conf. Comput. Vis. Pattern Recognit. (CVPR)*, pages 12853–12861, 2020.
- [41] Chi Zhang, Yujun Cai, Guosheng Lin, and Chunhua Shen. Deepemd: Few-shot image classification with differentiable earth mover’s distance and structured classifiers. In *Proc. IEEE Conf. Comput. Vis. Pattern Recognit. (CVPR)*, pages 12200–12210, 2020.